

Measurement of free-free emission from low-energy-electron collisions with Ar

C. Yamabe,* S. J. Buckman,[†] and A. V. Phelps[‡]

Joint Institute for Laboratory Astrophysics,

National Bureau of Standards and University of Colorado, Boulder, Colorado 80309

(Received 17 August 1982)

The production of free-free radiation in collisions of low-energy electrons with Ar atoms has been measured using the drift-tube technique. The excitation coefficients were obtained from measurements of the absolute intensity of continuum radiation at wavelengths of 500, 650, and 1300 nm. At 650 nm the electric-field-to-gas-density ratio E/N was varied from 0.25×10^{-21} to 10×10^{-21} V m² corresponding to mean electron energies from 1.2 to 5.4 eV. As expected, the emission was proportional to the argon density from 3×10^{24} to 15×10^{24} atoms/m³. The experimental excitation coefficients are in good agreement with calculations using theoretical free-free emission cross sections and electron energy distributions and serve to demonstrate the usefulness of simple formulas relating the free-free emission cross section to measured momentum-transfer cross sections.

I. INTRODUCTION

Interest in the emission of free-free radiation (bremsstrahlung) resulting from the collisions of low-energy electrons with rare-gas atoms has increased with the demonstration by Pfau and Rutscher¹ that free-free emission is responsible for much of the visible continuum emitted by rare-gas discharges. Other emission measurements using the discharge technique have been reported²⁻⁴ along with numerous measurements using the shock-tube technique.^{4,5} The inverse process of the absorption of radiation by free electrons has been of even greater interest because of the importance of this energy absorption and electron heating mechanism in the laser-induced breakdown of gases.⁶ Both of these topics have been investigated in great detail theoretically.⁶⁻¹³ Finally, there have been a number of recent experimental and theoretical investigations of narrow resonance structure in the free-free absorption cross section.¹³ Because of the narrow width and relatively small integrated contribution of these resonances to the averaged free-free cross sections of significance in our relatively low-energy resolution experiments, we will not be concerned with these features.

The present measurements of free-free emission were carried out using the electron drift-tube technique which we have used previously¹⁴⁻¹⁶ for measurements of excitation coefficients for weakly radiating states of molecules. In these experiments a photoelectrically produced electron current drifts through the gas under the action of a spatially uniform time-modulated electric field. About one in 10^8 collisions of the electrons with the gas atoms results in the emission of a visible photon. A small

fraction (~ 1 in 10^4) of these photons is selected by wavelength and reaches the sensitive area of the detector. The absolute photon flux is compared with that from a standard lamp, and the ratio is used to calculate the excitation coefficient. The principal advantage of the present technique over the discharge technique used in previous experiments¹⁻⁴ is that the electric field E and gas density N can be easily varied and accurately determined and that the theory of the experiment need not take into account electron-electron and electron-ion collisions.¹⁷ A disadvantage of the drift-tube technique is that the emitted intensities are about 10^4 smaller than in a typical discharge experiment.

The theory of the experiment and the experimental apparatus are briefly reviewed in Secs. II and III. The results are presented in Sec. IV and discussed in Sec. V.

II. THEORY OF EXPERIMENT

In this section we briefly review the results of theoretical calculations of free-free radiation and of the excitation coefficients which are relevant to this experiment. We then derive the equations necessary to relate the observed signals to the excitation coefficients.

A. Free-free emission theory

For our purposes it is convenient to divide the free-free emission continuum into a number of spectral bands of frequency width $d\nu$ and to regard the collision process leading to emission of radiation in this band as an inelastic collision between the electrons and gas atoms. The spectral intensity I_ν in units of photons per unit volume and per unit fre-

quency interval and per unit time is given by¹

$$I_\nu d\nu = n_e N \frac{d\nu}{\nu} \int_0^\infty \nu Q_{ff}(\epsilon, h\nu) \epsilon^{1/2} f(\epsilon) d\epsilon$$

$$\equiv k_{ff}(\nu) n_e N \frac{d\nu}{\nu}. \quad (1)$$

Here n_e and N are the electron and neutral atom or molecular densities, ν and ϵ are the electron speed and energy, $f(\epsilon)$ is the normalized electron energy distribution, and $Q_{ff}(\epsilon, h\nu)$ and k_{ff} are the cross section and rate coefficient per fractional bandwidth $d\nu/\nu$ for emission of a photon of energy $h\nu$ by the free-free process. Figure 1 shows theoretical calculations of the cross section per fractional bandwidth $Q_{ff}(\epsilon, h\nu)$ as obtained by a variety of theoretical approaches for $h\nu = 1.78$ eV. The dashed and solid curves are from the quantum-mechanical calculations of Ashkin¹⁰ and of Geltman.¹¹ The solid circles are our calculations using the very simple formula of Kas'yanov and Starostin⁸ for $h\nu \ll \epsilon$ and momentum-transfer cross sections used previously¹⁵ for Ar. This formula is

$$Q_{ff}(\epsilon, h\nu) = \frac{4}{3\pi} \frac{\alpha^3}{\text{Ry}} \frac{(\epsilon - h\nu/2)(\epsilon - h\nu)^{1/2}}{\epsilon^{1/2}} \times Q_m(\epsilon)$$

$$= 1.211 \times 10^{-8} \left[1 - \frac{h\nu}{2\epsilon} \right] \times \left[1 - \frac{h\nu}{\epsilon} \right]^{1/2} \epsilon Q_m(\epsilon), \quad (2)$$

where α is the fine-structure constant (1/137), Ry is the Rydberg (13.6 eV), ϵ is in eV, and $Q_m(\epsilon)$ is the cross section for momentum-transfer collisions of electrons with the atom or molecule. Calculations made using the formula of Holstein⁹ and the total and momentum-transfer cross sections of Hayashi¹⁸ are shown by the triangles in Fig. 1. The differences among the various theoretical cross sections shown in Fig. 1 are less than 30% over most of the electron energy range. Most of the difference between the cross section calculated using Eq. (2) and those calculated using Holstein's formula results from the fact that in Eq. (2) the Q_m is evaluated at ϵ , whereas in Holstein's formula the cross sections are evaluated at $\epsilon - h\nu/2$. The differences among the cross sections are larger near threshold, e.g., a factor of 3 at 2 eV for Ashkin's results versus our application of Holstein's formula shown in Fig. 1. The large differences between the calculations at electron energies above 20 eV are caused by differences in the momentum-transfer cross sections used in Ref. 15 and those of Hayashi.¹⁸ As we shall see, our experiments are not sensitive to cross sections at either of these extremes of energy. The cross sections predicted using the older formula of Firsov and Chibisov⁷ and the total scattering cross sections of Hayashi are much larger than the values shown in Fig. 1.

Excitation coefficients for free-free emission were calculated from the cross sections generated by Eq. (2), by Geltman,¹¹ and by the Holstein formula.⁹ The electron energy distributions for Eq. (1) are calculated using the numerical procedures of Frost and Phelps¹⁹ and the cross sections discussed by Tachibana and Phelps.¹⁴ The calculated free-free emission coefficients will be presented with the experimental results in Sec. IV. Although not directly useful in this paper because of the assumed Maxwellian electron energy distribution, we note that there is good agreement among a number of theoretical calculations^{4,11,12} of free-free emission and absorption coefficients for electrons in Ar. The Maxwellian electron energy distributions are appropriate to shock-tube experiments⁵ and to discharge experiments at high fractional ionization.²

It is important to keep in mind that throughout

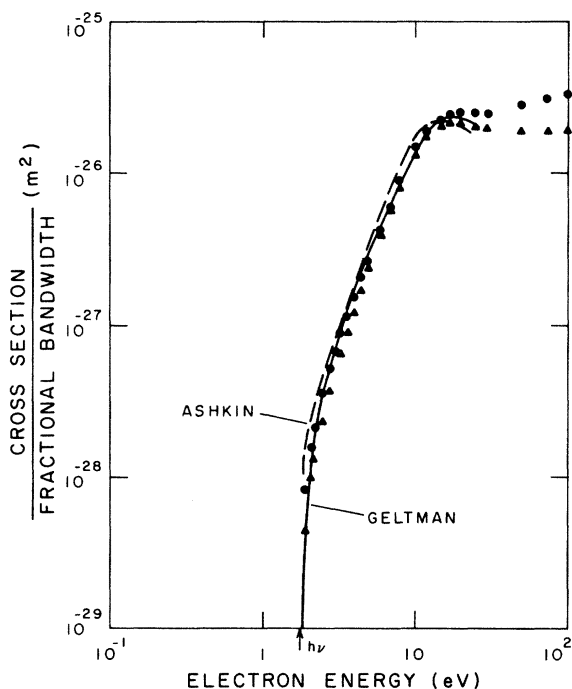


FIG. 1. Theoretical cross section per fraction bandwidth for the emission of 1.78-eV photons vs electron energy. The solid and dashed curves are from Geltman (Ref. 11) and Ashkin (Ref. 10), respectively. The circles and squares are our calculations based on the formulas of Kas'yanov and Starostin (Ref. 8) and of Holstein (Ref. 9), respectively.

this paper we have not followed the usual convention of expressing the free-free emission in terms of a spectral intensity, i.e., cross section or excitation coefficient per unit spectral bandwidth, but rather have defined cross sections and rate coefficients per fractional bandwidth. This unconventional formulation has the advantages of yielding numbers which are independent of units used to measure bandwidth and of yielding cross sections and excitation coefficients which are readily compared with cross sections and excitation coefficients for the production of excited states which emit lines or molecular bands. In our experiments the fractional bandwidth of the detection system is typically 0.1.

B. Model of experiment

The signal produced by the photon detector S_{ff} is obtained by integrating Eq. (1) over the drift-tube volume V and over frequency ν , taking into account the optical system and detector characteristics, i.e.,

$$S_{ff} = \int \int \frac{d\nu}{\nu} dV k_{ff}(\nu) n_e N f_w(\nu) D(\nu) \times f_i(\nu) \frac{\Delta Q_c}{4\pi} \eta(\vec{r}), \quad (3)$$

where $f_w(\nu)$ is the fractional transmission of the windows between the collision chamber and the detector, $D(\nu)$ is the responsivity per photon of the detector, amplifier, and recording system as a function of ν , $f_i(\nu)$ is the fractional transmission of the interference or other filter inserted between the collision chamber and the detector, ΔQ_c is the solid angle of the detector as seen from the center of the collision chamber, and $\eta(\vec{r})$ is the efficiency of the detection system at various points in the collision chamber relative to that at the center of the chamber.¹⁴

Equation (3) can be rewritten as

$$S_{ff} = \frac{N \Delta \Omega_c}{4\pi} \int_0^\infty f_w(\nu) k_{ff}(\nu) D(\nu) f_i(\nu) \frac{d\nu}{\nu} \times \int_V n_e \eta(\vec{r}) dV. \quad (4)$$

We define a geometrical factor G_{ff} by the relation

$$G_{ff} = \int_V n_e \eta(\vec{r}) dV / \int_V n_e dV. \quad (5)$$

We note that G_{ff} is equal to the G factor defined by Lawton and Phelps¹⁴ in the limit of no diffusion. Since ionization and attachment can be neglected in the present experiments at low E/N in pure Ar, the electron density n_e can be assumed to be independent of position in the electric-field direction. If, as

in previous papers,^{14,15} we neglect the effects of radial variations in the electron density, then the expression for G_{ff} reduces to a constant equal to the average of $\eta(\vec{r})$ over the active portion of the drift tube. This constant was 0.97 for the infrared detector and 0.80 for the photomultiplier detector.

In the usual case of a slow variation in f_w , $k_{ff}(\nu)$, and $D(\nu)$ with ν compared to that of $f_i(\nu)$, the integral over ν in Eq. (4) can be written as

$$f_w(\nu_i) k_{ff}(\nu_i) D(\nu_i) \langle f_i \rangle \Delta \nu.$$

Here $\langle f_i \rangle \Delta \nu$ is the "area" under the filter transmission curve, and ν_i is the photon frequency at the peak of the transmission of the interference filter. Equation (4) can now be approximated by

$$S_{ff} = \frac{N \Delta \Omega_c G_{ff}}{4\pi} \frac{iL}{ew_e} f_w(\nu_i) k_{ff}(\nu_i) D(\nu_i) \times \langle f_i \rangle \frac{\Delta \nu}{\nu}, \quad (6)$$

where L is the separation of the cathode and anode of the drift tube, i is the current through the drift tube, and e and w_e are the electron charge and drift velocity. Note that because of the absence of significant attachment or ionization, the q factor of Ref. 14 is equal to unity and so is omitted from Eq. (6). Measurements at significantly higher E/N would require that corrections be made for ionization. From Eq. (6) we note that since the free-free emission signal increases with the fractional bandwidth $\Delta \nu/\nu$ of the detection system, one should use a wide bandwidth interference filter or a very low-resolution monochromator for wavelength selection.

The reference signal S_r reaching the detector from the reference, i.e., the blackbody or the calibrated tungsten strip lamp, is given by

$$S_r = \Delta \Omega_r a_r \int_0^\infty f_r(\nu) f_w(\nu) \epsilon(\nu) B(\nu) \times D(\nu) f_i(\nu) d\nu, \quad (7)$$

where $\Delta \Omega_r$ is the solid angle of the detector as seen from a limiting aperture¹⁴ of area a_r , $f_r(\nu)$ is the transmission of the windows between the references source and the collision chamber, $\epsilon(\nu)$ is the emissivity of the references source, and $B(\nu) d\nu$ is the number of photons per second omitted by a blackbody per unit of surface and per unit solid angle. As discussed in Ref. 14, the reference sources were large enough to completely fill their limiting apertures as seen from the detector.

Using Eqs. (4), (5), and (7) rather than Eq. (6) for greater accuracy, we find that the ratio of the free-free emission signal to the reference signal is

$$\frac{S_{ff}}{S_r} = \frac{N \Delta \Omega_c G_{ff}}{4\pi \Delta \Omega_r a_r} \frac{iL}{ew_e} \frac{\int_0^\infty f_w(\nu) k_{ff}(\nu) D(\nu) f_i(\nu) d\nu/\nu}{\int_0^\infty f_r(\nu) f_w(\nu) \epsilon(\nu) B(\nu) D(\nu) f_i(\nu) d\nu}. \quad (8)$$

If we define a free-free excitation coefficient $\alpha_{ff}(\lambda_i)$ by

$$\alpha_{ff}(\lambda_i) = k_{ff}(v_i)N/w_e, \quad (9)$$

then

$$\frac{\alpha_{ff}(\lambda_i)}{N} = \frac{C_{ff}S_{ff}}{G_{ff}iNS_r}, \quad (10)$$

where here λ_i is taken to be the mean wavelength transmitted by interference filter and

$$C_{ff}(\lambda_i) = \frac{4\pi \Delta\Omega_r e a_r}{\Delta\Omega_c L} \frac{\int_0^\infty f_r(\lambda) f_w(\lambda) \epsilon(\lambda) B'(\lambda) D'(\lambda) f_i(\lambda) d\lambda}{\int_0^\infty f_w(\lambda) f_i(\lambda) \left[\frac{k_{ff}(c/\lambda)}{k_{ff}(c/\lambda_i)} \right] D'(\lambda) \frac{hc}{\lambda^2} d\lambda}. \quad (11)$$

Here

$$D'(\lambda) = D(\nu)/h\nu$$

and

$$h\nu B(\nu) d\nu = B'(\lambda) d\lambda.$$

Equation (11) was used for analyzing the data presented in this paper. We note that the formula for determining $\alpha_{ff}(\lambda_i)/N$ from the experimental data, i.e., Eq. (10), is very much like Eq. (17) of Lawton and Phelps¹⁴ for determining α_b/N for the metastable $O_2(b^1\Sigma)$ molecules.

III. EXPERIMENTAL APPARATUS AND PROCEDURE

A schematic of the drift-tube technique used for determination of the free-free excitation coefficients is shown in Fig. 2. Ultraviolet radiation from a continuously operating 100-W high-pressure mercury lamp is passed through broad interference filters with maximum transmission at 190 nm and then through a quartz window coated on the inside with a semitransparent, cathode film of evaporated Pd-Au alloy. The resulting photoelectrons enter the

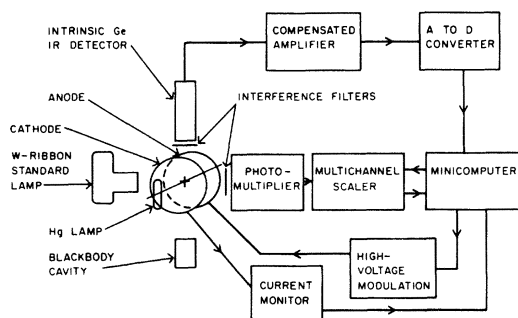


FIG. 2. Schematic of experiment. Note that the centers of the semitransparent cathode, the anode, the drift tube, and the Hg lamp are on an axis perpendicular to the plane of the reference sources and the detectors.

parallel-plate drift tube filled with Ar at densities in the range $(3-15) \times 10^{24}$ atom/m³. The anode voltage is modulated so as to periodically apply to a known electric field E and so produce electrons with a modulated mean energy. The photons emitted in the free-free transitions are detected with a photoconductive detector for the infrared or with a photomultiplier for visible wavelengths. The free-free emission signal is compared with the signal from a hollow cavity blackbody for the infrared and with a calibrated tungsten ribbon lamp for the visible wavelengths.

The drift tube used in these experiments and shown in the schematic of Fig. 2 is the same as the one used previously¹⁴⁻¹⁶ to measure excitation in molecular gases. The electrode spacing was 38.4 mm and the cathode diameter was 60 mm. The accelerating voltage ranged from 60 to 3100 V and the total current in the on-period was 0.02–0.09 μ A. Measurements are reported at total gas densities of $(3-15) \times 10^{24}$ m⁻³. Argon of nominal 99.999% purity was fed into the tube directly from a high-pressure cylinder.

A. Infrared system

The measurements at 1.3 μ m were made with a period of the zero-based square-wave voltage applied to the anode of 25 s as in the measurements of the 1.27- μ m emission from the $a^1\Delta_g$ state of O_2 . This data recording period was followed by a dead time of 15 s for computer processing of the data. The liquid-N₂ cooled, intrinsic germanium detector had responsivity and noise equivalent power (NEP) of 7×10^9 V/W and 1×10^{-15} W Hz^{-1/2}, respectively, at 1.3 μ m. The signal from the dc output of the detector for step function infrared input signal consists of rapidly and slowly rising components, the time constants of which were about 10 ms and 3 s, respectively. As described in Ref. 15, this problem was overcome by using an amplifier containing differentiation and addition circuits which compensate

for the 3-s response and partially compensate for the 10-ms response. The compensation circuits were adjusted for a square-wave output signal using the chopped signal from the blackbody as an input signal.

A minicomputer was used as a data acquisition and analyzing system. The signal from the compensated amplifier was sampled every 0.1 s using an analog-to-digital converter. A set of data was stored in the computer and then analyzed¹⁵ to reject spikes due to cosmic rays. Sixteen to thirty-two sets of data were additively accumulated and averaged in the computer.

The measurement of the sensitivity of the detection system for infrared radiation emitted from the center of the collision chamber was made using a blackbody source mounted on the opposite side of the drift tube from the detector. A chopper in front of the source modulated the blackbody emission with a period of 20 s. An aperture of 1.50-mm diameter was placed in front of the source 0.47 m from the detector so as to reduce the blackbody signal. When the temperature of the source was 490 K the intensity at the detector was comparable to that observed for the free-free emission and was large compared to the thermal background signal. The spatial variation of the detection efficiency $\eta(\vec{r})$ was measured using a small diffuse light source which was scanned over the drift region as described in Ref. 15.

B. Visible wavelength system

The detection system and reference light source for the measurements of free-free emission at 500 and 650 nm was a modification to that described by Lawton and Phelps.¹⁴ An improved photon counting system was used to integrate the photomultiplier signals during the on and off times for the high voltage applied to the drift tube. The photomultiplier counts and the digitized average cathode current were transferred to the minicomputer after a preset time interval. An interference filter with 68% transmission and a band pass of 68-nm full width at half maximum (FWHM) was used for the measurements reported for 500 nm. Measurements at 650 nm were made using an interference filter with 65% peak transmission and a band pass of 33-nm FWHM. As pointed out previously,¹⁴ the final results are insensitive to the magnitude of the interference filter transmission. The filter characteristics were measured separately using a commercial spectrophotometer. A multi-alkali-metal photomultiplier in a uv transmitting envelope with a slowly varying quantum efficiency between 250 and 800 nm was used with these filters. The principal diffi-

culty encountered in these measurements was that of the calibration of the neutral density filters used to reduce the signal from the standard lamp to values in the linear range of the photon counting system.

We estimate an uncertainty of $\pm 20\%$ for the resultant measured excitation coefficients for both the infrared and visible wavelengths. The significant changes in these estimates from those of Ref. 14 are the absence of a contribution to the uncertainty from a radiative lifetime, a more accurate measurement of the aperture area ($\pm 4\%$), and a more accurate determination of the electron current ($\pm 5\%$).

IV. FREE-FREE EMISSION DATA

In this section we summarize the results of measurements of the free-free emission coefficients for electrons in Ar. Figure 3 shows an example of the infrared emission signals which led us to the conclusion that the drift-tube technique could be used to measure free-free emission coefficients. This waveform was obtained during measurements of $O_2(a^1\Delta)$ production in a mixture of 0.05% O_2 in Ar at a total gas density of 10^{25} m^{-3} and an E/N of $3 \times 10^{-21} \text{ V m}^2$. The exponentially rising and falling portions of this waveform are interpreted as emission from $O_2(a^1\Delta)$ molecules at $1.27 \mu\text{m}$ and yield excitation coefficients consistent with those reported in Refs. 14 and 15. When the exponentially varying portions are subtracted from the observed waveform one is left with a rectangular waveform which we interpret as free-free emission emitted in collisions between electrons and argon atoms. This interpretation is supported by the fact that in pure Ar only the rectangular component of the waveform was observed. Although one expects the free-free emission signal to follow the rapid changes in the electron

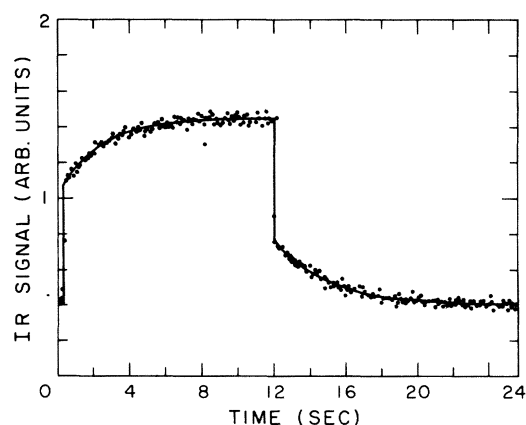


FIG. 3. Infrared emission transient near $1.3 \mu\text{m}$ from 0.05% O_2 in Ar.

density, we made no effort to observe the free-free emission with a time resolution better than the 0.1-s value normally used in the $O_2(a^1\Delta)$ experiments. Winkler, Michel, and Wilhelm²⁰ have observed changes in the free-free emission from afterglows in Ne and Ar on a microsecond time scale. The principal clues to the identity of the signal were the slow variation of the signal with E/N and with wavelength, as discussed in the remainder of this section.

The free-free emission coefficients for pure Ar at wavelengths near $1.3 \mu\text{m}$ are calculated from the observed magnitude of the infrared signal using Eqs. (10) and (11). The averages of several runs are shown as a function of E/N by the squares in Fig. 4. Similarly, the triangles and the circles of Fig. 4 show the averages of results of measurements near 500 and 650 nm , respectively. Plots of the free-free emission coefficient versus wavelength for E/N values of $3 \times 10^{-21} \text{ V m}^2$ (squares) and $2 \times 10^{-21} \text{ V m}^2$ (triangles) are shown in Fig. 5. Note that when appropriate corrections are made for the effects of attachment, the free-free emission data of Fig. 3 and other data from O_2 -Ar mixtures obtained during measurements at $1.3 \mu\text{m}$ are consistent with

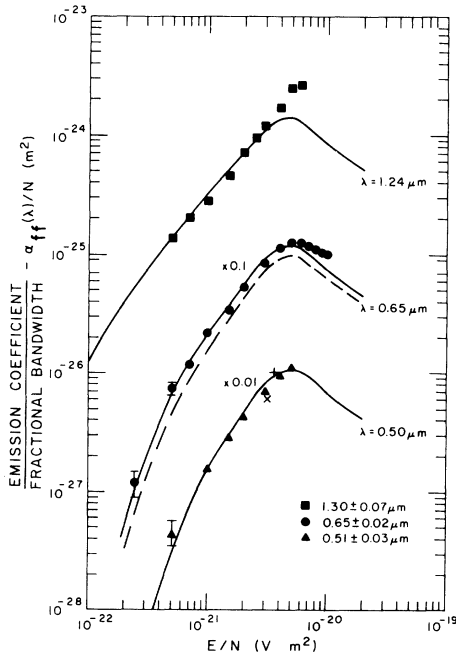


FIG. 4. Free-free emission coefficient per fractional bandwidth for electrons in argon vs E/N . The error bars shown at low E/N for 500 and 600 nm are the statistical uncertainties associated with photon counting. The \times and $+$ are representative data from Refs. 2 and 3, respectively. The solid curves represent calculated values obtained using Eqs. (1) and (2). The dashed curve shows results calculated using Holstein's formula (Ref. 15).

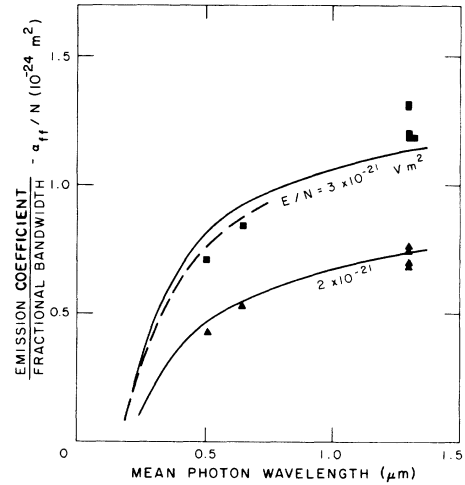


FIG. 5. Wavelength dependence of free-free emission coefficient per fractional bandwidth for electrons in Ar. The solid curves are our calculated values, while the dashed curve is from Pfau, Rutscher, and Winkler (Ref. 21). The triangles and squares are our experimental results for E/N values of 2 and $3 \times 10^{-21} \text{ V m}^2$, respectively.

the $1.3\text{-}\mu\text{m}$ data shown in Fig. 4.

The solid curves of Figs. 4 and 5 are the result of calculations of free-free emission coefficients which we have made using Eq. (2) for the free-free emission cross section and the electron energy distributions which we have calculated. For this purpose, it is convenient to write Eq. (1) as

$$\frac{\alpha_{ff}}{N} = \frac{k_{ff}}{w_e} = \frac{1}{w_e} \left(\frac{2}{m} \right)^{1/2} \int_{h\nu}^{\infty} \epsilon Q_{ff}(\epsilon) f(\epsilon) d\epsilon. \quad (12)$$

Here α_{ff} is the number of free-free photons emitted per unit distance of electron drift and per fractional bandwidth. According to Eq. (12) the normalized excitation coefficient is expected to be independent of the argon density. Our electron energy distributions were calculated using the electron-Ar collision cross-section data discussed in Sec. III and in Ref. 15. The dashed curve for $\lambda = 650 \text{ nm}$ of Fig. 4 was calculated using the $Q_{ff}(\epsilon, h\nu)$ values for $\lambda = 650 \text{ nm}$ calculated using the theory of Holstein. In this case the momentum-transfer cross section of Hayashi¹⁸ were used in the calculation of $f(\epsilon)$, although the $Q_m(\epsilon)$ values of Refs. 15 and 18 agree for $\epsilon < 3 \text{ eV}$ and differ by less than 10% for $\epsilon < 15 \text{ eV}$. The α_{ff}/N values calculated from the theoretical cross sections of Geltman are not shown in Fig. 4 since they differ from the results obtained with Eq. (1) by less than about 5% for $E/N > 0.3 \times 10^{-21} \text{ V m}^2$. The decrease in the calculated α_{ff}/N values for E/N greater than 4×10^{-21}

$V\text{ m}^2$ is the result of an increase in the slope of the drift velocity versus E/N data as well as a decrease in the slope of k_{ff} vs E/N at E/N where inelastic collisions are important.^{14,21} The calculated mean electron energies vary from 1.2 eV at $E/N = 2.5 \times 10^{-22} \text{ V m}^2$ to 5.4 eV at $E/N = 1 \times 10^{-20} \text{ V m}^2$. The dashed curve of Fig. 5 was obtained by interpolation of graphs of calculations by Pfau, Rutscher, and Winkler.²¹ The lower emission coefficients obtained by these authors compared to those we calculate at the same E/N appear to be the result of their use of somewhat larger $Q_m(\epsilon)$ values for electron-Ar collisions with a resultant lower mean electron energy and lower α_{ff}/N .

For E/N below $3 \times 10^{-21} \text{ V cm}^2$, the agreement between experiment and the theory of Kas'yanov and Starostin⁸ as shown by the solid curves is within $\pm 15\%$ or the statistical uncertainty of the data in spite of the fact that the $h\nu$ values are comparable with the photon energy. Although the theoretical curve calculated using the formula of Holstein⁹ lies well outside the statistical uncertainty of our data, it is just within the confidence limits we have assigned to our results. The relatively large experimental values and rapid increase of the α_{ff}/N coefficients relative to theory for $\lambda = 1.3 \mu\text{m}$ at E/N values about $4 \times 10^{-21} \text{ V m}^2$ are consistent with α/N values which we calculate for the emission of line radiation by highly excited Ar atoms. The excess of the measured signal at 650 nm at $E/N > 5 \times 10^{-21} \text{ V m}^2$ varies much less rapidly with E/N than expected for highly excited states of Ar. Although this discrepancy may indicate an error in the values of $Q_m(\epsilon)$ at electron energies above about 10 eV, further measurements of the spectral distribution of the radiation should be made as to verify that the emission at the higher E/N is free-free radiation.

Absolute measurements of free-free emission signals from electrical discharges in Ar are reported for wavelengths from 300 to 500 nm by Vasileva, Zhdanova, and Mnatsakanyan³ and for 480 nm by Golubovskii, Kagan, and Komarova.^{2,22} Their results were about $(75 \pm 20)\%$ and $(100 \pm 20)\%$, respectively, of their theoretical values. Representative experimental data obtained by these authors at 500 nm are shown in Fig. 4. The E/N range of their low current discharges sets the mean electron energy in the range of 4–5 eV. The agreement between experiment and theory shown for these authors is remarkably good when one considers the problems of the determination of the electron density and of the effects of gas heating on the analysis of their experimental data.²² The results of Vasileva *et al.*³ and of Rutscher and Pfau¹ also provide tests of the theoretical predictions of the wavelength dependence of the free-free emission.

V. DISCUSSION

The results presented in this paper show the usefulness of the electron drift-tube technique for the measurement of free-free emission coefficients for electrons in gases. This technique makes possible measurements of free-free emission coefficients under much more accurately known experimental conditions for a wide range for mean electron energies (1.2–5.4 eV) than was possible using the discharge technique. The free-free emission coefficients for photon energies between 1 and 2.5 eV and for mean electron energies between 1.7 and 5.0 eV agree with theoretical predictions to within $\pm 15\%$. At 650 nm and mean electron energies from 1.7 down to 1.2 eV the experimental and theoretical agree within the statistical uncertainty of less than $\pm 25\%$, while at mean electron energies above 5.0 eV the apparent discrepancy between theory and experiment increases with electron energy. Unfortunately, the mean electron energies required to produce a measurable signal are too large to enable us to work in the threshold electron energy range where the various theories are more easily distinguished. Measurements of free-free emission at very high densities of pure gases or absorption measurements using low mean energy electrons might make possible a choice from among the theories. Free-free emission measurements²³ at extremely high gas densities ($\sim 10^{29} \text{ m}^{-3}$) should provide data for testing theories appropriate to conditions in which the time between electron-atom collisions is comparable to the photon frequency but under much more accurately controlled conditions than in the laser breakdown experiments⁶ carried out at these densities. Such high-density emission experiments should provide a valuable complement to electron mobility measurements at high gas densities where departures from the binary collision model of electron scattering may occur.²⁴

On the basis of the success of the simple formula for calculating free-free emission coefficients for argon, one is encouraged to recommend the use of this formula for other gases for which the momentum-transfer cross section is known. Obviously, it would be desirable to test the formula against experiment for other gases, e.g., He and N_2 .

ACKNOWLEDGMENTS

The authors would like to thank Y.-M. Chan, S. Lissauer, E. R. Mosburg, Jr., H. Page, and R. T. Weppner for valuable help and advice during these experiments. One of us (A.V.P.) would like to acknowledge a number of helpful discussions of this problem with T. Holstein. This work was supported in part by the U.S. Air Force Wright Aeronautical Laboratories.

- *On leave 1980–1981 from Department of Electrical Engineering, Nagoya University, Nagoya 464, Japan.
- †Current address: Research School of Physical Sciences, Australian National University, Canberra, A.C.T. 2600, Australia.
- ‡Permanent address: Quantum Physics Division, National Bureau of Standards and Physics Department, University of Colorado, Boulder, Colorado 80309.
- ¹S. Pfau and A. Rutscher, *Z. Naturforsch.* **22a**, 2129 (1967); *Beitr. Plasmaphys.* **8**, 73 (1968); A. Rutscher and S. Pfau, *ibid.* **8**, 315 (1968); *Physica (Utrecht)* **81C**, 395 (1976).
- ²Yu. M. Kagan and N. N. Kristov, *Opt. Spektrosk.* **27**, 710 (1969) [*Opt. Spectrosc. (USSR)* **27**, 388 (1969)]; Yu. B. Golubovskii, Yu. M. Kagan, and L. L. Komarova, *ibid.* **34**, 226 (1973) [*ibid.* **34**, 127 (1973)]; **33**, 1185 (1972) [**33**, 646 (1972)].
- ³I. A. Vasileva, Yu. Z. Zhdavona, and A. Kh. Mnatsakanyan, *Opt. Spektrosk.* **29**, 664 (1970) [*Opt. Spectrosc. (USSR)* **29**, 345 (1970)].
- ⁴For a bibliography on free-free transitions in electrons collisions with atoms and molecules see J. W. Gallagher, Joint Institute for Laboratory Astrophysics Information Center Report No. 16, University of Colorado (unpublished).
- ⁵R. L. Taylor and G. Caledonia, *J. Quant. Spectrosc. Radiat. Transfer* **2**, 657 (1969); R. T. V. Kung and C. H. Chang, *ibid.* **16**, 579 (1976).
- ⁶C. G. Morgan, *Rep. Prog. Phys.* **38**, 621 (1975). Note that absorption measurements have been made under the much more controlled conditions of an electron beam sustained discharge in H₂ and N₂ by S. Alroy and W. H. Christiansen, *Appl. Phys. Lett.* **32**, 607 (1978). Also free-free transitions have been observed using laser radiation and monoenergetic electrons by D. Andrick and L. Langhans, *J. Phys. B* **9**, L459 (1976).
- ⁷O. B. Firsov and M. I. Chibisov, *Zh. Eksp. Teor. Fiz.* **39**, 1770 (1960) [*Sov. Phys.—JETP* **12**, 1235 (1961)].
- ⁸V. Kas'yanov and A. Starostin, *Zh. Eksp. Teor. Fiz.* **48**, 295 (1965) [*Sov. Phys.—JETP* **21**, 193 (1965)].
- ⁹T. Holstein (private communication) and as quoted in Ref. 10. Equations (18) and (19) of Ref. 10 are too large by a factor of 2. Note that when Holstein's formula is used with Ashkin's total and momentum-transfer cross sections the agreement with Ashkin's Q_{ff} is very good.
- ¹⁰M. Ashkin, *Phys. Rev.* **141**, 41 (1966).
- ¹¹S. Geltman, *J. Quant. Spectrosc. Radiat. Transfer* **13**, 601 (1973). We are indebted to S. Geltman for tables of free-free transition matrix elements, which were interpolated to obtain the cross-section values shown.
- ¹²T. L. John and A. R. Williams, *J. Phys. B* **6**, L384 (1973); M. S. Pindzola and H. P. Kelly, *Phys. Rev. A* **14**, 204 (1976). See however, J. R. Stallcop, *Astron. Astrophys.* **30**, 293 (1974).
- ¹³M. Gavrilina and M. van der Wiel, *Comments At. Mol. Phys.* **8**, 1 (1978); H. Krüger and M. Schulz, *J. Phys. B* **9**, 1899 (1976). Resonance structure in the free-free scattering of electrons has been observed by L. Langhans, *J. Phys. B* **11**, 2361 (1978).
- ¹⁴S. A. Lawton and A. V. Phelps, *J. Chem. Phys.* **69**, 1055 (1978).
- ¹⁵K. Tachibana and A. V. Phelps, *J. Chem. Phys.* **75**, 3315 (1981).
- ¹⁶C. Yamabe and A. V. Phelps, *J. Chem. Phys.* (in press).
- ¹⁷L. M. Biberman and G. E. Norman, *Usp. Fiz. Nauk.* **91**, 193 (1967) [*Sov. Phys. Usp.* **10**, 52 (1967)].
- ¹⁸Recommended momentum transfer and total cross sections for several gases are given by M. Hayashi, Institute of Plasma Physics, Nagoya University, Report No. IPPJ-AM-19 (unpublished).
- ¹⁹L. S. Frost and A. V. Phelps, *Phys. Rev.* **127**, 1621 (1962); **136**, A1538 (1964).
- ²⁰R. Winkler, P. Michel, and J. Wilhelm, *Beitr. Plasmaphys.* **18**, 31 (1978).
- ²¹S. Pfau, A. Rutscher, and R. Winkler, *Beitr. Plasmaphys.* **16**, 317 (1976).
- ²²The data shown in Fig. 4 from Ref. 2 are those for which electron-electron collisions effects are negligible, i.e., for the largest value of pR and the smallest value of i/R in their notation.
- ²³Evidence for free-free emission has been obtained from measurements of electroluminescence from scintillation counters filled with Xe at densities near $6 \times 10^{26} \text{ m}^{-3}$ and operated at E/N of less than $5 \times 10^{-23} \text{ V m}^2$. See Yu. A. Butikov, B. A. Polgoshein, V. N. Lebedenko, A. M. Rogozhin, and B. V. Rodionov, *Zh. Eksp. Teor. Fiz.* **57**, 42 (1969) [*Sov. Phys.—JETP* **30**, 24 (1970)].
- ²⁴V. M. Atrazhev and I. T. Yakubov, *Teplofiz. Vys. Temp.* **18**, 1292 (1980) [*High Temp. (USSR)* **18**, 966 (1980)]; G. L. Braglia and V. Dallacasa, in *Electron and Ion Swarms*, edited by L. G. Christophorou (Pergamon, New York, 1981), p. 83; G. R. Freeman, *ibid.*, p. 93.